Supplementary Material (ESI) for Journal of Materials Chemistry

Electronic Supplementary Information

Morphology-Controlled Synthesis of Highly Adsorptive Tungsten Oxide Nanostructures and Application to Water Treatment

*By Seongho Jeon and Kijung Yong**

Surface Chemistry Laboratory of Electronic Materials, Department of Chemical Engineering, POSTECH (Pohang University of Science and Technology), Pohang, 790-784, Korea

E-mail: kyong@postech.ac.kr

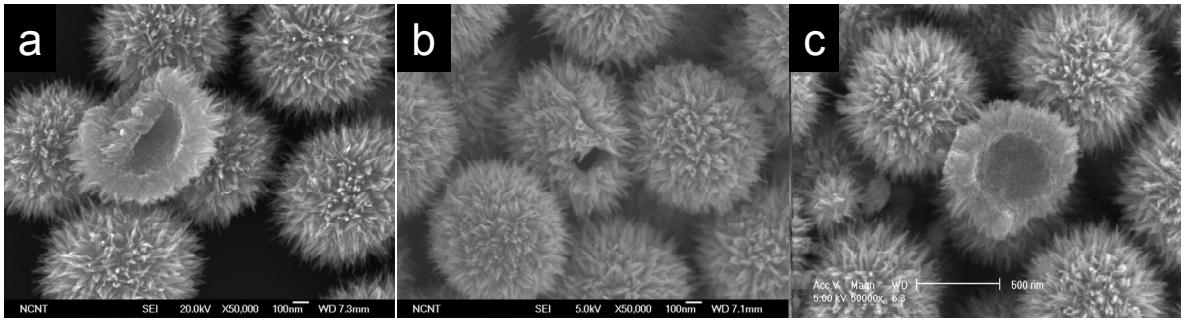

Figure S1. SEM images of the fractured products synthesized at 200°C after 24 h reaction time by solvothermal reaction of 11.36 mM of $W(CO)_6$ solution.

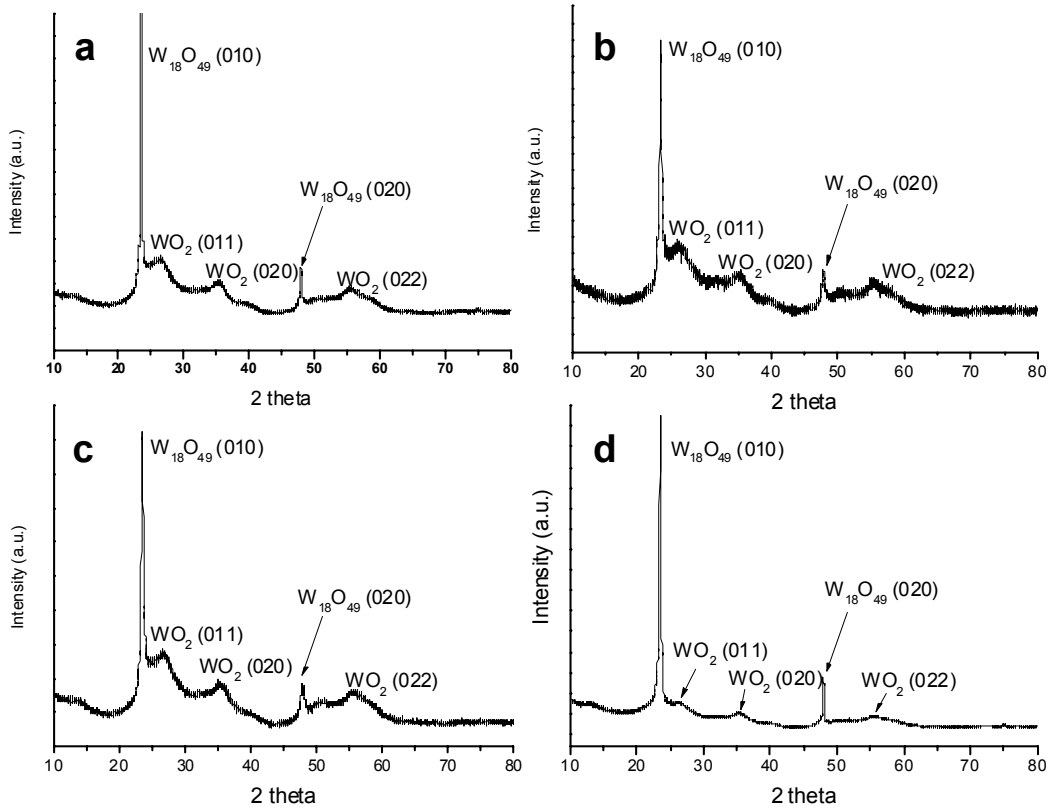

Figure S2. XRD patterns of the as-prepared products prepared with different concentrations of $W(CO)_6$: (a) 28.4 mM, (b) 11.36mM, (c) 7.1 mM, (d) 4.26 mM.

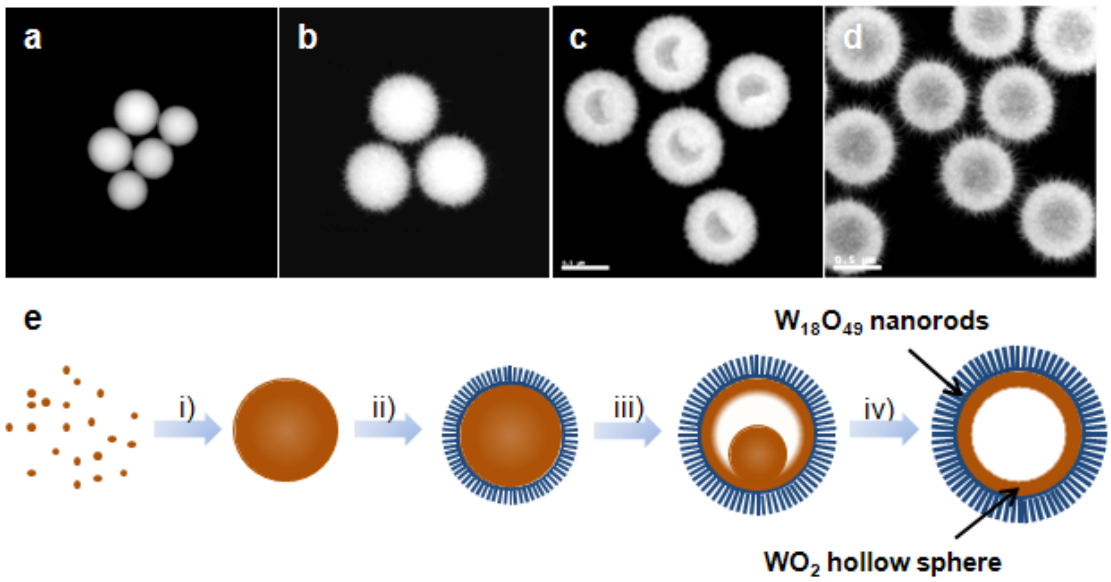

Figure S3. (a)–(d) HAADF-STEM images of the products obtained at 200°C for different reaction times: (a) 20 min; (b) 1 h; (c) 5 h; (d) 24 h and (e) schematic illustration of the formation mechanism for the composite $W_{18}O_{49}/WO_2$ hollow urchins: (i) In the initial stages, the small amorphous WO_2 nanoparticles formed quickly, then spontaneously aggregated into large spheres to minimize the overall energy of the system; (ii) As the reaction proceeded, the reaction rate slowed due to the depletion of the reactants. As a result, the crystal growth stage transferred to a kinetically controlled process. Subsequent crystal growth was initiated on the surfaces of the spheres, and the $W_{18}O_{49}$ nanorods were epitaxially grown on the surfaces due to their propensity for one-dimensional growth; (iii) Because the surface layer of the WO_2 spheres was crystalline due to contact with the surrounding solution and was stabilized by the outer layer of $W_{18}O_{49}$ nanorods, the amorphous core underneath the crystalline surfaces tended to dissolve, leading to sphere-in-sphere structured WO_2 particles; iv) The nanorods located on the outer surface may have acted as the starting points for subsequent crystallization processes using the dissolved core materials. The subsequent crystal growth tended to be epitaxial and, finally, formed composite $W_{18}O_{49}$ nanorods/WO_2 hollow spheres (i.e. composite hollow urchins).

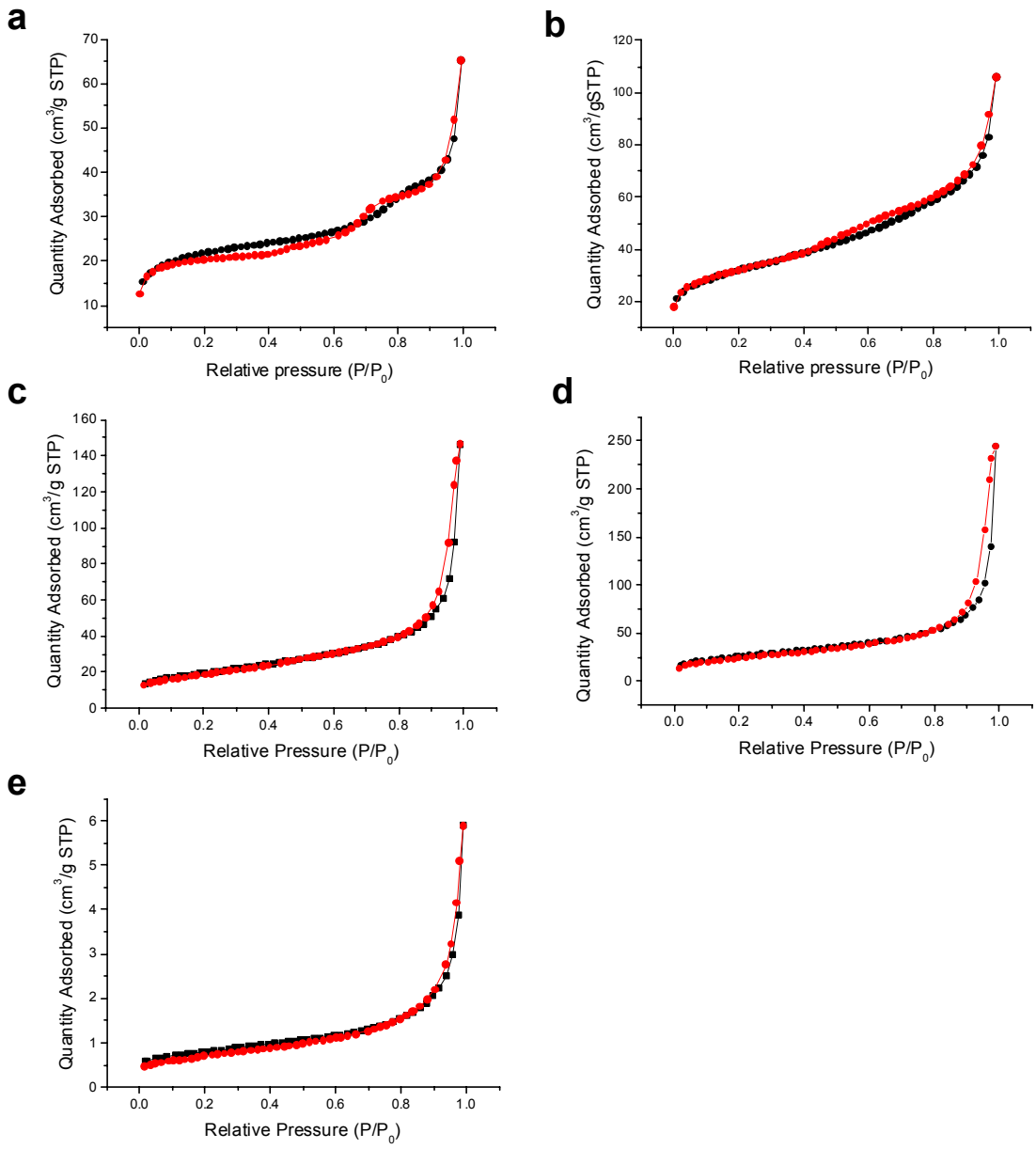

Figure S4. N_2 adsorption/desorption curves of tungsten oxide nanostructures prepared at different concentrations of $W(CO)_6$: (a) 28.4 mM, (b) 11.36 mM, (c) 7.1 mM, (d) 4.26 mM. (e) N_2 adsorption/desorption curves of commercial tungsten oxide powder.

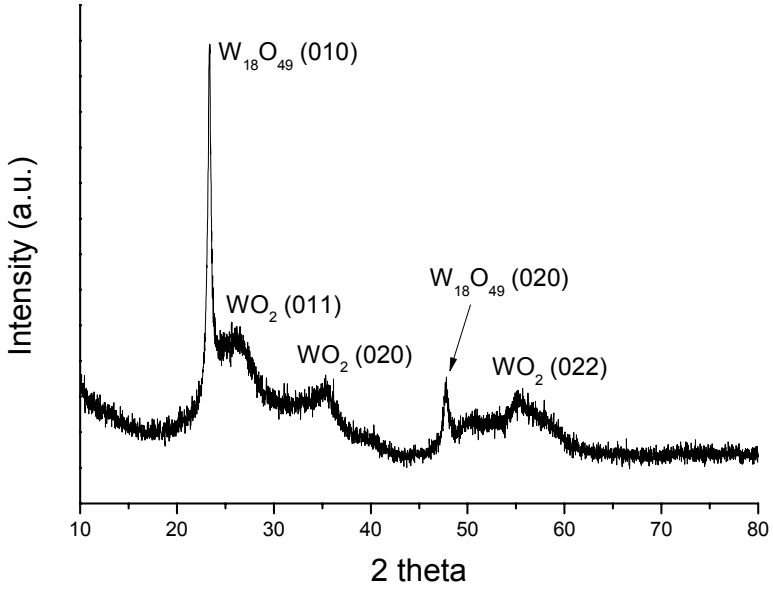

Figure S5. XRD patterns of the regenerated products via 300°C air annealing for 3h.